Systemic glycerol decreases neonatal rabbit brain and cerebellar growth independent of intraventricular hemorrhage

Christopher M. Traudt[1], Ron J. McPherson[1], Colin Studholme[1], Kathleen J. Millen[1] and Sandra E. Juul[1]

BACKGROUND: Cerebellar hypoplasia is a common problem in preterm infants and infants suffering from intraventricular hemorrhage (IVH). To evaluate the effects of IVH on cerebellar growth and development, we used a neonatal rabbit model of systemic glycerol to produce IVH.

METHODS: New Zealand White rabbit kits were surgically delivered 2 d preterm and treated with intraperitoneal glycerol (3.25–6.5 g/kg). Controls were born at term. IVH was documented by ultrasonography. Brain volumes determined by magnetic resonance imaging, cerebellar foliation, proliferation (Ki-67), and Purkinje cell density were assessed at 2 wk of life. Tissue glycerol and glutathione concentrations were measured.

RESULTS: Glycerol increased IVH, subarachnoid hemorrhages, and mortality in a dose-dependent manner. Total cerebellar volumes, cerebellar foliation, and cerebellar proliferation were decreased in a dose-dependent manner. Glycerol accumulated rapidly in blood, brain, and liver and was associated with increased glutathione concentration. All of these results were independent of IVH status.

CONCLUSION: Cerebellar hypoplasia was induced after glycerol administration in a dose-dependent manner. Given the rapid tissue accumulation of glycerol, dose-dependent decrease in brain growth, and lack of IVH effect on measured outcomes, we question the validity of this model because glycerol toxicity cannot be ruled out. A better physiological model of IVH is needed.

Although mortality of preterm infants weighing less than 1,000 g is decreasing, up to 50% of preterm survivors have cognitive, learning, social, behavioral, and motor deficits (1,2). Cerebellar hypoplasia has recently been documented in preterm infants with poor neurological outcomes (3–5). The cerebellum increases in size by almost fivefold between 24 and 40 wk postconceptual age, making it vulnerable to both developmental disruption and injury (6). Risk factors associated with cerebellar hypoplasia in preterm infants include intraventricular hemorrhage (IVH), hemosiderin deposition, periventricular leukomalacia, hypoperfusion from patent ductus arteriosus, low pH in first 5 d of life, low bicarbonate levels, and chorioamnionitis (6,7). The mechanisms of injury from these insults are not known.

IVH increases the risk of poor outcome in the absence of other injuries (8). One hypothesis of cerebellar hypoplasia following IVH is that blood mixes with the cerebral spinal fluid and coats the cerebellum (9,10). Subsequent breakdown of blood may disturb communication between the proliferative external granular layer (EGL) of the cerebellum and the overlying meningeal tissues, resulting in disruption of normal cerebellar lamination (9,11). Evidence in support of this hypothesis comes from magnetic resonance imaging (MRI) studies showing siderosis of hypoplastic cerebellum in infants with history of IVH (12,13).

To examine the effects of IVH on cerebellar development, we used the previously described rabbit model of systemic glycerol–induced IVH (14,15). In this model, the proposed mechanism of brain injury begins when systemic glycerol produces a decrease in intracranial pressure, which is followed by a reperfusion that produces germinal matrix hemorrhage with extension into the lateral ventricles (16). Because the effect of IVH on cerebellar development has not been characterized, we adopted this model to confirm its usefulness for understanding cerebellar hypoplasia following IVH in preterm infants. We hypothesized that glycerol-induced IVH would decrease EGL proliferation and produce cerebellar hypoplasia.

RESULTS

All neonatal rabbits (100%) injected with intraperitoneal glycerol developed subarachnoid hemorrhages (SAHs) within 2 h of injection. We observed these SAHs through the skin overlying the skull. In **Figure 1a**, we have incised and retracted the skin to show the extent of SAH visible through the skull. **Figure 1** also shows examples of ultrasound images from a glycerol-treated animal with no detectable IVH (**Figure 1b**) and **a** glycerol-treated animal with IVH (**Figure 1c**). Data for prevalence of SAH, IVH, and mortality are listed in **Table 1**. Mortality was defined as death before 2 wk of age. Mortality and IVH rates increased with increasing glycerol dose. Postmortem examination did not reveal pneumonia or other signs of infection, but we did observe cases of dilated intestines and discolored

[1]Department of Pediatrics, University of Washington, Seattle, Washington; Correspondence: Christopher M. Traudt (ctraudt@uw.edu)

Received 20 June 2013; accepted 7 August 2013; advance online publication 8 January 2014. doi:10.1038/pr.2013.236

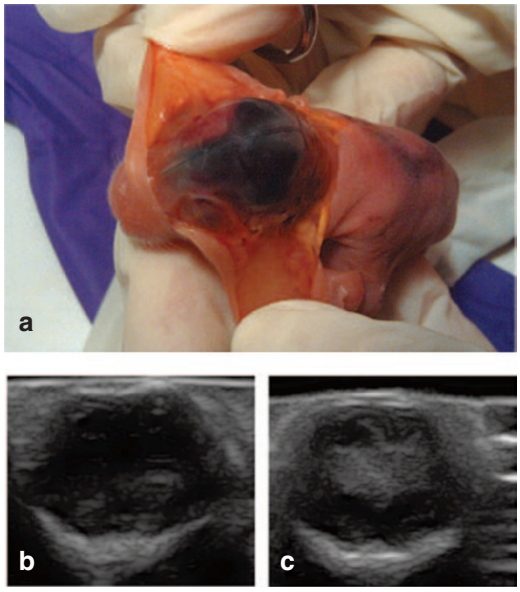

Figure 1. Intracranial hemorrhages after glycerol. (**a**) A killed neonatal rabbit kit is held with skin retracted to expose the skull, which shows the subarachnoid hemorrhage that is always present after glycerol injection. At 24 h after glycerol injection, coronal ultrasound scans were collected to document the presence of intraventricular hemorrhage (IVH). (**b**) An ultrasound image from an animal with no indication of IVH and (**c**) an ultrasound image from an animal with large IVH present 24 h after glycerol injection.

Table 1. Prevalence of SAH, IVH, and mortality in neonatal rabbits treated with different doses of systemic glycerol

Glycerol dose (g/kg)	0	3.25	4.87	6.5
Number, *N*	34	18	4	28
SAH at 2 h, % (*N*)	0	100 (18)**	100 (4)**	100 (28)**
IVH at 24 h, % (*N*)	0	22 (4)	50 (2)	46 (13)
Mortality, % (*N*)	18 (6)	61 (11)*	25 (1)	82 (23)**

IVH, intraventricular hemorrhage; SAH, subarachnoid hemorrhage.

Kruskal–Wallis test with Dunn's multiple comparison test: *$P \le 0.01$ or **$P \le 0.001$, compared with control animals (0 g/kg dose).

organs. No seizures or evidence of increased intracranial pressures were noted. SAH did not predict subsequent IVH because only a fraction of animals exhibited IVH when examined with ultrasonography 24 h after glycerol injection. The sizes of IVHs at 24 h varied from small (ventricle only) to large (ventricle and parenchyma). In all three glycerol-treated animals with IVH that survived 2 wk, posthemorrhagic hydrocephalus was present at necropsy.

Brain volume was evaluated by *ex vivo* MRI ($N = 18$). Interrater reliability of brain segmentation was determined by Dice similarity coefficients. The Dice similarity coefficients among the three tracers ranged from 0.931 to 0.998. Glycerol reduced total brain and cerebellar volumes in a dose-dependent manner (**Figure 2**) independent of presence of IVH. To evaluate cerebellar growth, we examined the histology shown in **Figure 3**, which includes lamination of the cerebellum, proliferation of the EGL, and Purkinje cell density in a subset of animals ($N = 11$). **Table 2** quantifies cerebellar indexes, such as foliation (lobes I–III perimeter); primary

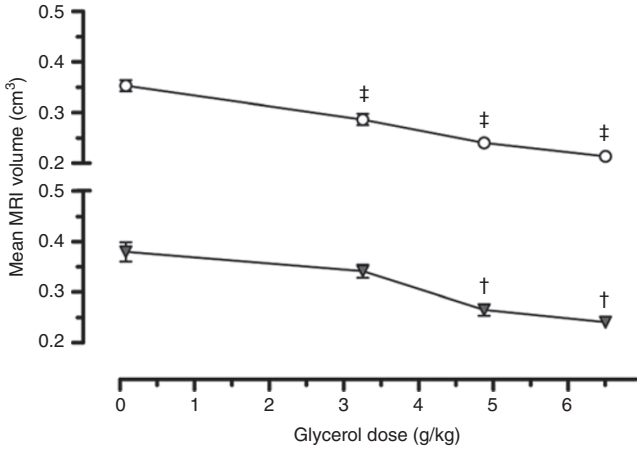

Figure 2. Line plots showing dose-dependent decreases in total brain (unfilled circle) and cerebellum (filled triangle) volumes (means ± SEM) of the rabbits observed using magnetic resonance imaging (MRI). Premature rabbit kits were delivered by Caesarean section and treated with glycerol at the doses indicated; then, 2 wk after treatment, kits were killed and the brains were perfusion fixed and removed for subsequent MRI measurements ($N = 3$–5 per dose). ANOVA differences compared with 0-dose control are indicated as follows: ‡$P \le 0.001$ and †$P \le 0.05$ (Dunnett's *post hoc* tests). MRI volumes did not correlate with the presence of intraventricular hemorrhage.

fissure length (distance to first lobule of lobe V); and internal granular, molecular, and EGL thicknesses, as well as Ki-67-immunopositive proliferation and Purkinje cell density. In the EGL, glycerol treatment decreased cerebellar foliation complexity, size, and EGL thickness and reduced cell proliferation (indicated by decreased Ki-67 immunolabeling). Note that the increase in Purkinje cell density in the 6.5 g/kg glycerol group is likely a secondary effect of decreased cerebellar growth. All of these effects of glycerol were dose related but unrelated to IVH status.

Because glycerol treatment affected cerebellar development and brain growth without producing IVH, we investigated *post hoc* the possibility that glycerol may accumulate in tissues to produce direct toxic effects. **Figure 4** illustrates that 1 h after systemic injection (6.5 g/kg), glycerol concentrations increased more than 240-fold in plasma, more than 30-fold in the hippocampus and cerebellum, and more than 60-fold in liver; moreover, glycerol remained elevated in tissues for at least 6 h. Finally, the total glutathione concentration in cortical brain tissue was elevated by 13% at 1 h and by 27% at 6 h after glycerol injection.

DISCUSSION

The key findings of our study are as follows: (i) there is a glycerol dose–dependent increase in IVH; (ii) there is a glycerol dose–dependent decrease in total brain and cerebellar volumes, which are independent of IVH; (iii) posthemorrhagic hydrocephalus is caused by glycerol injection although the mechanism has not been elucidated; (iv) cerebellar proliferation and foliation are decreased; and (v) glycerol rapidly accumulates in tissues, including the brain. We also found this model to be difficult to work with due to high mortality rates and the inconsistent rates and severity of IVH.

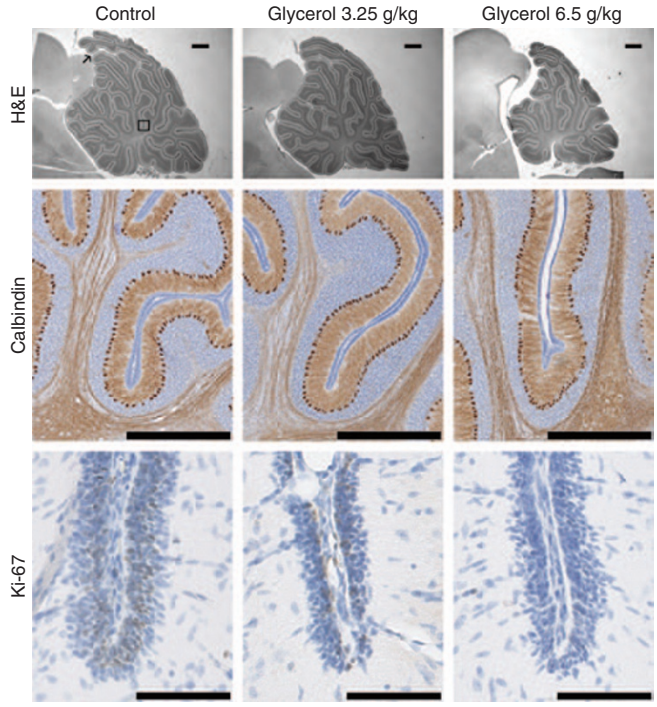

Figure 3. Photomicrographs showing the dose-dependent effects of systemic glycerol treatment on cerebellar development. Brain sections from control (left column) and glycerol-treated (right columns) rabbit kits were stained with hematoxylin and eosin (H&E; top row; bar = 1 mm); staining for calbindin-D28K (middle row; bar = 800 µm) and Ki-67 (bottom row; bar = 90 µm). Measurements were made along the primary fissure of the vermis, as denoted in the upper left panel by the thin black arrow marking the start and by the black box marking the end of the region of interest. Cerebellar growth was compromised because the density of calbindin-immunopositive Purkinje cells was increased and the proportion of Ki-67-immunopositive proliferating external granular layer (EGL) cells (thick black arrows) was decreased in glycerol-treated kits. Morphological measurements using H&E-stained images indicated that the foliation is less complex, and the thickness of the EGL is decreased at the base of the primary fissure in glycerol-treated kits.

Table 2. Histological indexes describing cerebellar development in neonatal rabbits treated with/without systemic glycerol

	Dose of glycerol (g/kg)		
	0	3.25	6.5
Number, *N*	4	4	3
Lobes I–III perimeter (mm)	29.1 ± 2.7	24.2 ± 1.6	19.8 ± 1.1*
Primary fissure length (µm)	1,345 ± 71	1,031 ± 46**	810 ± 35***
Internal granular layer thickness (µm)	69.5 ± 2.0	64 ± 5.6	74.1 ± 2.6
Molecular layer thickness (µm)	171 ± 4	143 ± 9	166 ± 8
EGL thickness (µm)	35.5 ± 4.4	18.9 ± 2.8***	26.2 ± 3.1*
Purkinje cell density (% total area)	0.287 ± 0.003	0.285 ± 0.013	0.319 ± 0.008*
Ki-67 immunolabeling (% total area)	0.627 ± 0.122	0.452 ± 0.121	0.125 ± 0.060*

EGL, external granular layer.

Data are presented as means ± SEM. Kruskal–Wallis test with Dunn's multiple comparison test were performed for the Purkinje density and Ki-67 positivity. ANOVA with Dunnett's *post hoc* comparisons with control (0 g/kg dose) was used for the remaining parameters: $*P \le 0.05$, $**P \le 0.01$, $***P \le 0.001$.

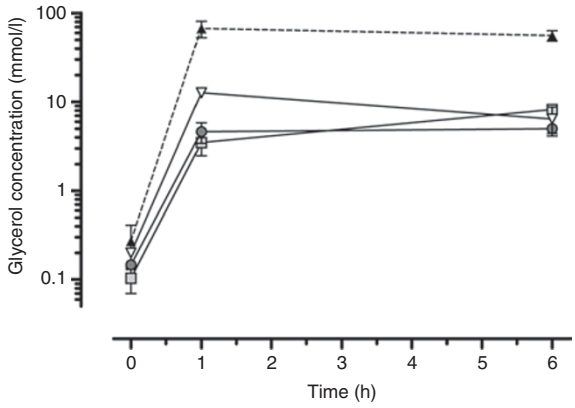

Figure 4. Line plots showing that glycerol is elevated more than 240-fold in blood plasma and elevated more than 30- to 60-fold in tissues at 1 and 6 h after glycerol administration (data ± SEM). Glycerol concentrations are plotted on a logarithmic scale for plasma (filled triangle), hippocampus (light gray square), cerebellum (dark gray circle), and liver (unfilled triangle). Newborn rabbits, untreated (time 0) or glycerol treated (6.5 g/kg intraperitoneal), were killed at 1 or 6 h posttreatment and samples of brain and liver tissue were collected, snap frozen, and then homogenized and assayed for glycerol content by enzyme-linked immunosorbent assay ($N = 3$ per time point). Subarachnoid hemorrhages were evident shortly after injection, but no intraventricular hemorrhages were detected after brain removal.

Our findings may be contrasted with those from previous reports that used systemic glycerol in neonatal rabbits. For example, our neonatal rabbit mortality was double the 30% rate reported previously (14) and, in many cases, the cause of death was uncertain as thriving kits were simply found dead with no evidence of aspiration or IVH at necropsy. One potential cause of death would be acute renal failure because systemic injection of 50% glycerol is known to produce a nephrotoxicity similar to that due to rhabdomyolysis (17,18). Although previous reports found that glycerol produced similar rates of prevalence for SAH (75%) and IVH (70–80%) (14,15), we found that these two effects did not correspond. When present, we observed considerable variation in the size of IVH identified by ultrasonography. Thus, it appears that IVH produced by systemic glycerol is infrequent, inconsistent, and variable, and together, these findings confirm the observation that the frailty of newborn rabbits and inconsistency of IVH diminish the value of this model (19). One limitation of our study is that we did not measure intracranial pressures. Previous studies found that glycerol lowered intracranial pressure in a dose-dependent manner (16,20).

Cerebral growth was decreased after glycerol injection independent of IVH status. MRI measures of forebrain and cerebellar volumes, and measurements of cerebellar morphometry, identified dose-dependent effects of glycerol on brain growth. A number of proliferative processes may be affected by glycerol treatment (21,22). For example, glycerol disrupts maturation of oligodendrocyte precursors, and this may reduce overall brain growth (14). Although we did not measure cerebral perfusion,

it is unlikely that the global impairment of brain growth was due to glycerol-induced hypoperfusion (16). Given the universal presence of SAH, it is possible that SAH, but not IVH, is a contributing factor in the retardation of brain growth. In hamsters, SAH interferes with responses in meninges and related proliferation signals and reduces proliferation in the EGL (11). Similarly, glycerol acts directly to disrupt membrane and cytoskeletal proteins that thereby interfere with cellular interactions that mediate normal brain growth (23).

Toxins that disturb cell proliferation during development are particularly detrimental. Cerebellar development is a prolonged process during which progenitor cells of the EGL proliferate, migrate, and differentiate continuously for up to 2 postnatal mo in rabbits or for 7 postnatal mo in humans (24–26). Thus, there is a large window of vulnerability during which this developmental sequence may be disrupted. In this study, a single injection of glycerol decreased cerebellar MRI volume and decreased foliation of the primary fissure. Both cell proliferation (Ki-67) and laminar width were decreased in the EGL. The decreased proliferation seen 14 d postinjection is likely the principal mechanism underlying reduced cerebellar growth and may also indicate that glycerol-mediated toxicity is enduring. The coincident increase in Purkinje cell density that we observed is probably secondary to decreased foliation and reduced cerebellar area with relative preservation of Purkinje neurons. Alternatively, increased Purkinje density could occur as an artifact of histological processing if brain edema were present *in vivo*. Recently, it was determined that cerebellar neuronal granule cells are actually derived from astroglia that generate granule cell precursors (27). Given the proximity of the EGL to the meninges and the prolonged period of postnatal cerebellar development, it is possible that the cerebellum is particularly susceptible to the toxic effects of glycerol and/or SAH. Our data certainly support this hypothesis.

It is apparent that glycerol may produce brain toxicity directly in the absence of IVH. Systemic glycerol (6.5 g/kg) rapidly accumulated in blood, liver, and brain tissues. We acknowledge that this effect was not detected when the dose of glycerol was 1.15 g/kg (28). Notably, the progressive accumulation of total glutathione content in brain is an indication that a single injection of systemic glycerol alters cerebral biochemistry independent of IVH. This is problematic because it appears that IVH cannot be reliably produced unless a high dose of glycerol is administered and, at high doses, direct toxic effects of glycerol cannot be disqualified as an alternative explanation for any resulting brain injury.

For infants born prematurely, neurological complications arise when the capillaries of the immature germinal matrix lose their integrity and produce IVH and subsequent ventricular dilatation (29). Glycerol is highly lipophilic and can be used *in vitro* to lyse cells (30) and, when used as a cryoprotectant, glycerol is known to disrupt the integrity of the membrane and the actin cytoskeleton of spermatozoa (31,32). Because our study indicates that glycerol readily penetrates brain tissues, perhaps glycerol produces cerebral hemorrhage by directly lysing susceptible endothelial membranes, including those in the germinal matrix.

In conclusion, the validity of the use of the systemic glycerol to model neonatal IVH is questionable for several reasons. First, the mortality due to this treatment is high, possibly due to known renal toxicity. Second, although this treatment reliably produces SAH, IVH is inconsistent and variable. Third, the design cannot disqualify the alternative interpretation that brain injury resulting from systemic injection of glycerol is mediated by direct toxic action. A better model of spontaneous IVH still needs to be found, given that organotypical brain slices exposed to whole blood exhibited pathophysiological changes in the absence of glycerol (33).

METHODS

Animals

All experimental protocols were approved by the Animal Care and Use Committees at the University of Washington in accordance with the US National Institutes of Health guidelines. Timed-pregnant New Zealand White does (Western Oregon Rabbit, Philomath, OR) were purchased ($N = 13$). On embryologic day 29, the doe was sedated with isoflurane for a nonsurvival Caesarean section ($N = 9$). The preterm kits ($N = 63$) were extracted from the uterus, dried, and placed in an incubator prewarmed to a temperature of 35 °C. Control kits ($N = 34$) were delivered vaginally at term.

Brain Injury

Preterm kits were injected with 3.25, 4.87, or 6.5 g/kg of glycerol intraperitoneally (Sigma Chemical, St. Louis, MO), given as a 50% solution (by volume) at 2 h of age to induce IVH (15).

Feeding

Kits were hand-fed twice daily with a commercial rabbit milk substitute formulated to support neonatal rabbit growth (Fox Valley Animal Nutrition, Sun City, AZ), supplemented with 60 g/l lyophilized colostrum (Naturade, Orange, CA). Commercial nipples (Chris's Squirrels and More, LLC, Somers, CT) were used. For the first 2 d, kits were fed 100 ml/kg/d, and thereafter, the feeding volumes increased gradually to 280 ml/kg/d.

Ultrasonography

Cranial ultrasonography was performed at 24 h of age to document presence of IVH using a SonaScape S8 with 10–5 MHz L743 linear array probe (SonoScape, Shenzhen, China).

MRI Acquisition

At 12 d postterm, surviving kits were killed. Rabbit brains were extracted after perfusion fixation and placed in Multihance (Bracco Diagnostics, Princeton, NJ) 1:100 in phosphate-buffered saline for 28 d. Brains were then placed in Fomblin (Solvay Solexis, West Deptford, NJ) for *ex vivo* imaging ($N = 17$) on Bruker Avance III 14 Tesla (600) (Bruker, Fremont, CA) Ultrashield high-resolution 89-mm vertical bore magnet with ParaVision version 5.1 software (ParaVision, Fremont, CA). The TurboRARE T2 sequence with a scan time of 7.5–8 h was acquired with the following settings: field of view: 2.82 cm; slice thickness: 0.11 mm, interslice distance: 0.11 mm, slices: 256, axial slice orientation matrix P1: 256; repetition time: 27,807 ms, echoes: 1, echo time (TE) effective 1: 33 ms, TE effective 2: 33 ms; averages: 30; field of view read: 2.82 cm, field of view P1: 2.82 cm, matrix read: 256, matrix P1: 256; anti-alias read: 1, anti-alias P1: 1; resolution read: 0.011 cm/pixel, resolution read P1: 0.011 cm/pixel; iso distance: 1.6 mm, pack extent: 28.16 mm, scheme: interlaced, readout: L–R; repetition time: 27,807 ms, echoes: 1, TE effective 1: 33 ms, TE effective 2: 33 ms, averages: 30, bandwidth 1: 39682.5, flip back: on, fat suppression: on, rare partitions: 8.

Volumetric Analyses

RView software (Seattle, WA; http://rview.colin-studholme.net/) (34) was used for volume rendering of T2-weighted images. Structures were isolated using voxel-based intensity thresholds with manual limits. Tracings were performed by C.M.T. and two students (Henry Smelser and Olivia Janson) blinded to treatment group. Specific boundaries for total brain and cerebellum were defined. Total brain volume included the cerebral hemispheres, diencephalon, brainstem, and cerebellum. Ventricular cerebrospinal fluid was excluded, the

brainstem was truncated posterior to the area postrema, and the optic bulbs were excluded anterior to the fissura rhinalis (35). Final images were rendered in three-dimensional form and inspected for accuracy before structural volumes were computed.

Morphometric Measurements of Cerebellum

After MRI, the brains were imbedded in paraffin, and sagittal sections 10 μm thick were obtained. Using ImageJ software (National Institutes of Health), the perimeter of lobes I–III was outlined on hematoxylin and eosin–stained images of sagittal slices through the vermis. The distance from the primary fissure sulcus to the first branch point of lobe V was measured along the internal granule layer. The thickness of the internal/external granule and the molecular layers was measured at the primary fissure sulcus.

Immunohistochemistry

All staining procedures were run on the Leica Bond Automated Immunostainer with Leica bond kits (Leica Microsystems, Buffalo Grove, IL). Slides were baked for 30 min at 60 °C and deparaffinized. Antigen retrieval comprised citrate or EDTA treatment for 20 min at 100 °C. Slides were blocked in normal donkey serum (10% in Tris-buffered saline) for 10 min at room temperature. Primary antibodies mouse anti-human Ki-67 clone E3 ubiquitin-protein ligase MIB1 (1:1,000, Dako North America, Carpinteria, CA) or mouse anti-chicken calbindin (1:10,000; Swant, Marly, Switzerland) were applied at room temperature for 30 min. Leica goat anti-mouse horseradish peroxidase polymer was applied for 30 min at room temperature and blocked with peroxide for 10 min. Leica bond mixed (3, 3'-diaminobenzidine) refine detection was applied twice for 10 min at room temperature. Slides were counterstained with hematoxylin.

Slides were scanned using a Nanozoomer Digital Pathology slide scanner (Olympus America; Center Valley, PA). The digital images were then imported into Visiopharm software (Hoersholm, Denmark) for analysis. Using the Visiomorph Digital Pathology module, regions of interest were applied around relevant areas using a tissue detect protocol and manual cleanup. The software was then programmed to label positively stained areas vs. normal tissue areas, using project-specific configurations created for each staining set in a blinded manner. Images were processed in batch using these configurations to generate the desired output calculations.

Glycerol Accumulation in the Brain

Tissue glycerol concentrations were measured in a subset of kits killed at 0, 1, or 6 h after injection of 6.5 mg/kg of glycerol. The kits were killed, and plasma was obtained by heart puncture before exsanguination with heparinized saline. The brain was maintained on ice while the hippocampus and cerebellum were excised. The hippocampus, cerebellum, and liver samples were then frozen in liquid nitrogen. The tissues were homogenized in a 50:50 mixture of chloroform and methanol. Tissue supernatant and plasma were extracted and processed for glycerol concentration using a glycerol assay (BioAssay Systems, Hayward, CA) per assay instructions.

Antioxidant Status

The total glutathione content was measured using a commercial competitive assay (OxiSelect Total Glutathione Assay Kit; Cell Biolabs, San Diego, CA) on cortex tissue samples obtained at 0, 1, and 6 h after glycerol injection. Samples were homogenized per assay instructions. After centrifugation, the supernatant was diluted 1:100 and the assay was performed. Results were normalized to the 0-h time point and expressed as a percentage change.

Statistics

Results are given as mean ± SEM. Mortality was defined as death before 12 d postterm. Kruskal–Wallis testing with Dunn's multiple comparison test and ANOVA with Dunnett's *post hoc* comparisons were performed using SPSS. All glycerol-treated animals were randomized in a blinded fashion and all data were also analyzed in a blinded fashion.

ACKNOWLEDGMENTS

We thank Sarah Rammeli, Olivia Janson, and Henry Smelser for animal care work and data gathering, and Olivia Janson and Henry Smelser for MRI tracing.

STATEMENT OF FINANCIAL SUPPORT

We acknowledge financial support for this work from the National Institutes of Health 5K12HD043376-10; the University of Washington Neonatology: Neonatal Bioresearch Fund, Seattle, WA; and the University of Washington Neonatology Divisional funds, Seattle, WA.

Disclosure: The authors do not have any financial or conflicts of interest to report.

REFERENCES

1. Doyle LW, Anderson PJ. Adult outcome of extremely preterm infants. Pediatrics 2010;126:342–51.
2. Marlow N, Wolke D, Bracewell MA, Samara M; EPICure Study Group. Neurologic and developmental disability at six years of age after extremely preterm birth. N Engl J Med 2005;352:9–19.
3. Johnsen SD, Bodensteiner JB, Lotze TE. Frequency and nature of cerebellar injury in the extremely premature survivor with cerebral palsy. J Child Neurol 2005;20:60–4.
4. Limperopoulos C, Benson CB, Bassan H, et al. Cerebellar hemorrhage in the preterm infant: ultrasonographic findings and risk factors. Pediatrics 2005;116:717–24.
5. Steggerda SJ, Leijser LM, Wiggers-de Bruïne FT, van der Grond J, Walther FJ, van Wezel-Meijler G. Cerebellar injury in preterm infants: incidence and findings on US and MR images. Radiology 2009;252:190–9.
6. Limperopoulos C, Soul JS, Gauvreau K, et al. Late gestation cerebellar growth is rapid and impeded by premature birth. Pediatrics 2005;115:688–95.
7. Messerschmidt A, Prayer D, Brugger PC, et al. Preterm birth and disruptive cerebellar development: assessment of perinatal risk factors. Eur J Paediatr Neurol 2008;12:455–60.
8. Mercier CE, Dunn MS, Ferrelli KR, Howard DB, Soll RF; Vermont Oxford Network ELBW Infant Follow-Up Study Group. Neurodevelopmental outcome of extremely low birth weight infants from the Vermont Oxford network: 1998-2003. Neonatology 2010;97:329–38.
9. Tam EW, Miller SP, Studholme C, et al. Differential effects of intraventricular hemorrhage and white matter injury on preterm cerebellar growth. J Pediatr 2011;158:366–71.
10. Inage YW, Itoh M, Wada K, Hoshika A, Takashima S. Glutamate transporters in neonatal cerebellar subarachnoid hemorrhage. Pediatr Neurol 2000;23:42–8.
11. von Knebel Doeberitz C, Sievers J, Sadler M, Pehlemann FW, Berry M, Halliwell P. Destruction of meningeal cells over the newborn hamster cerebellum with 6-hydroxydopamine prevents foliation and lamination in the rostral cerebellum. Neuroscience 1986;17:409–26.
12. Castro Conde JR, Martínez ED, Rodríguez RC, Rodríguez De Hoyos AL. CNS siderosis and dandy-walker variant after neonatal alloimmune thrombocytopenia. Pediatr Neurol 2005;32:346–9.
13. Messerschmidt A, Brugger PC, Boltshauser E, et al. Disruption of cerebellar development: potential complication of extreme prematurity. AJNR Am J Neuroradiol 2005;26:1659–67.
14. Chua CO, Chahboune H, Braun A, et al. Consequences of intraventricular hemorrhage in a rabbit pup model. Stroke 2009;40:3369–77.
15. Georgiadis P, Xu H, Chua C, et al. Characterization of acute brain injuries and neurobehavioral profiles in a rabbit model of germinal matrix hemorrhage. Stroke 2008;39:3378–88.
16. Conner ES, Lorenzo AV, Welch K, Dorval B. The role of intracranial hypotension in neonatal intraventricular hemorrhage. J Neurosurg 1983;58:204–9.
17. Korrapati MC, Shaner BE, Schnellmann RG. Recovery from glycerol-induced acute kidney injury is accelerated by suramin. J Pharmacol Exp Ther 2012;341:126–36.
18. Rieger E, Rech VC, Feksa LR, Wannmacher CM. Intraperitoneal glycerol induces oxidative stress in rat kidney. Clin Exp Pharmacol Physiol 2008;35:928–33.
19. Coulter DM, LaPine T, Gooch WM 3rd. Intraventricular hemorrhage in the premature rabbit pup. Limitations of this animal model. J Neurosurg 1984;60:1243–5.

20. Cantore G, Guidetti B, Virno M. Oral glycerol for the reduction of intracranial pressure. J Neurosurg 1964;21:278–83.
21. Wiebe JP, Dinsdale CJ. Inhibition of cell proliferation by glycerol. Life Sci 1991;48:1511–7.
22. Sugiyama N, Mizuguchi T, Aoki T, et al. Glycerol suppresses proliferation of rat hepatocytes and human HepG2 cells. J Surg Res 2002;103:236–42.
23. Dinsdale CJ, Mirza FM, Wiebe JP. Glycerol alters cytoskeleton and cell adhesion while inhibiting cell proliferation. Cell Biol Int Rep 1992;16:591–602.
24. Lossi L, Ghidella S, Marroni P, Merighi A. The neurochemical maturation of the rabbit cerebellum. J Anat 1995;187 (Pt 3):709–22.
25. Smith KR Jr. The cerebellar cortex of the rabbit. an electron microscopic study. J Comp Neurol 1963;121:459–83.
26. Sidman RL, Rakic P. Neuronal migration, with special reference to developing human brain: a review. Brain Res 1973;62:1–35.
27. Silbereis J, Heintz T, Taylor MM, et al. Astroglial cells in the external granular layer are precursors of cerebellar granule neurons in neonates. Mol Cell Neurosci 2010;44:362–73.
28. Waterhouse JM, Coxon RV. The entry of glycerol into brain tissue. J Neurol Sci 1970;10:305–11.
29. Whitelaw A. Periventricular hemorrhage: a problem still today. Early Hum Dev 2012;88:965–9.
30. Bautista ML, Altaf W, Lall R, Wapnir RA. Cord blood red cell osmotic fragility: a comparison between preterm and full-term newborn infants. Early Hum Dev 2003;72:37–46.
31. Macías García B, Ortega Ferrusola C, Aparicio IM, et al. Toxicity of glycerol for the stallion spermatozoa: effects on membrane integrity and cytoskeleton, lipid peroxidation and mitochondrial membrane potential. Theriogenology 2012;77:1280–9.
32. Check ML, Check JH, Long R. Detrimental effects of cryopreservation on the structural and functional integrity of the sperm membrane. Arch Androl 1991;27:155–60.
33. Vinukonda G, Hu F, Upreti C, et al. Novel organotypic *in vitro* slice culture model for intraventricular hemorrhage of premature infants. J Neurosci Res 2012;90:2173–82.
34. Jacob FD, Habas PA, Kim K, et al. Fetal hippocampal development: analysis by magnetic resonance imaging volumetry. Pediatr Res 2011;69(5 Pt 1):425–9.
35. Shek JW, Wen GY, Wisniewski HM. Atlas of the Rabbit Brain and Spinal Cord, 1st edn. Basel, NY: Karger, 1986:1–139.